

Intramolecular proton transfer in adenine imino tautomers

S. SAHA[†], F. WANG^{†*} and M. J. BRUNGER[‡]

[†]Centre for Molecular Simulation, Swinburne University of Technology, PO Box 218, Hawthorn, Melbourne, Vic. 3122, Australia

[‡]School of Chemistry, Physics and Earth Sciences, Flinders University, GPO Box 2100, Adelaide, SA 5001, Australia

(Received July 2006; in final form October 2006)

The electronic structural impact on intramolecular proton transfer in the *cis*- and *trans*-imino N7 and N9 tautomers of adenine (A) has been studied quantum mechanically, using density functional theory (B3LYP/TZVP, SAOP/TZ2P, LB94/TZ2P) and Green function (OVGF/TZVP) models. It is found that proton transfer does not significantly change isotropic properties but has profound impact on electron distributions of the species through anisotropic properties. The relative energies with respect to the canonical A tautomer (amino-9H), ΔE , for imino 7H*cis*, imino 7H*trans*, imino 9H*cis* and imino 9H*trans* are calculated as 16.15, 16.43, 18.46 and 13.80 kcal mol⁻¹ (B3LYP/TZVP model) and some minor changes in perimeters of the purine ring is also observed. The Hirshfeld atomic charges indicate that whether a proton attached to N₍₇₎ or N₍₉₎ causes a significant local charge redistribution. However, these charges are insensitive to *cis*–*trans* proton transfer. Condensed Fukui function reveals N₍₁₀₎ and C₍₈₎ as the most electrophilic reactive site among N- and C-atom sites, respectively. We also found that proton transfer significantly alters in-plane σ orbitals, rather than out of plane π orbitals including the frontier orbital 6a^{''}. Moreover, orbital based responses to various proton transfers are presented: the orbital 29a['] (HOMO-1) is a signature orbital differentiating all the four tautomers. Orbital 27a['] is a site (N₍₇₎ and N₍₉₎) sensitive orbital, whereas orbital 22a['] is only sensitive to proton orientation on the imino group =N–H.

Keywords: Proton transfer; Adenine tautomers; Momentum distribution; Hirshfeld charge; Condensed Fukui function

1. Introduction

Tautomeric transitions of DNA bases are proton transfer reactions, which play an important role in biology. Indeed, Watson and Crick [1] suggested a mechanism for the spontaneous occurrence of these transitions in a classic paper on the DNA double helix. For example, adenine (A), the topic of the present work, can be alkylated by cancer chemotherapeutics as well as environmental mutagens, thereby damaging the genome [2]. In this regard, it was noted [3–5] that some of the hydrogen atoms on each of the four bases can change their location to produce a tautomer due to ionizing radiation, which mismatches the bases in their canonical form. This in turn lead to breaks in the backbone and formation of cross-covalent linkage between bases on the same or opposite strand. The substitution of one base pair for another is a common type of mutation. For example, mis-incorporation of A and cytosine (C) can occur when they are in a rare imino tautomeric form rather than the favoured amino tautomers [6]. In particular, imino C will pair with amino A, and imino A will pair with amino C.

Unusual tautomeric forms of bases [7] have been found in damaged DNA duplex, indicating that the transition to such alternative forms is indeed feasible [8,9]. A tautomers can be produced by two means: the proton on the N₍₉₎ position (the most stable position in amino-A [10]) shifts to one of the available N positions, such as the N₍₇₎ position in the purine ring. Alternatively, one of the protons in the amino group, –NH₂, of A relocates to other available N sites in the purine ring, creating the *cis*–*trans* imino forms (=NH) depending on the proton orientation. The existence of other A tautomers is further evidenced by experimental studies [11–14], often in the presence of a metal [15]. For example, the existence of tautomeric forms of A in complexes with transition metal ions was revealed by Rubina *et al.* [16]. It was also found that the A imino tautomer is more stabilized under the influence of charged platinum cations [17]. However, this preference was eliminated for the neutral PtCl₂(NH₃) adduct, giving a similar energy difference between the imino- and amino-forms of A as found in the case of non-metalized A tautomers. Plützer and Kleinermanns [18] demonstrated the coexistence of the A amino N9 and amino N7

*Corresponding author. Email: fwang@swin.edu.au

tautomers in an IR absorption spectrum of A in gas phase. As a result, A imino tautomers with proton transferred in *cis-trans* and N9/N7 pairs are studied in present work.

Any single procedure for studying tautomeric behaviour is not necessarily the “best” for all purposes [19]. Tautomers do not exhibit significant differences in terms of their ground electronic state total energies and geometries [20,21], but do exhibit significant electron density redistributions as reflected by anisotropic properties such as dipole moments [21,22]. To reveal properties of tautomers appropriately, one therefore needs approaches, which are sensitive to anisotropic changes. For example, we recently developed a dual space analysis (DSA) technique [23] which bridges qualitative interpretation power (e.g. for molecular orbital contours, dipole moments and Hirshfeld charges, etc.) with a quantitative prediction potential (e.g. Fourier transformed orbital momentum distributions (MDs) in momentum space), to study orbital based tautomeric and conformational processes of some biomolecules [6,22,24,25]. Here, we extend that earlier work to report our most recent results on configurational variation and electronic structural changes, in response to the proton transfer in *cis* and *trans* imino A tautomers of N7 and N9, using Hirshfeld atomic charges, dipole moments, condensed Fukui functions and orbital MDs.

2. Method and computational details

Four A imino *cis* and *trans* tautomers, that is, imino 7H*cis*, imino 7H*trans*, imino 9H*cis* and imino 9H*trans*, all confined on the molecular plane (imposing C_s symmetry) [21], were optimized using the same hybrid density functional theory (DFT) B3LYP/TZVP model as in Ref. [21]. As our purpose is to generate reliable orbital ionization energies for the tautomers, theoretical models such as DFT, -SAOP/TZ2P [26,27], -LB94/TZ2P [28] and an outer valence Green’s function (OVGF) [29] model are employed based on single point calculations of the optimized geometry of the B3LYP/TZVP model. All calculations are performed using the GAUSSIAN03 package of computational chemistry programs [30], except for LB94/TZ2P and SAOP/TZ2P which uses the ADF [31] programs.

For the properties in coordinate space, Hirshfeld atomic charges [32], molecular dipole moments and condensed Fukui functions [33], based on the LB94/TZ2P model, are generated. The Hirshfeld charge is determined by the integral of the partial electron density associated with atom A, excluding the corresponding nuclear charge Z_A, as [32]:

$$Q_A^H = Z_A - \int \frac{\rho_A^0(r)}{\sum_X \rho_X^0(r)} \cdot \rho(r) dr.$$

where $\rho(r)$ is the molecular electron density, $\rho_A^0(r)$ the isolated atomic electron density (spherically averaged,

ground state) of atom A and $\sum_X \rho_X^0(r)$ the sum over the electron densities of atoms present at their position in the molecule (referred as the promolecule density). This approach is based on the idea of describing the molecule by dividing it into its constituent atoms and seeing how these atoms differ from the isolated atoms [34].

The Fukui function, which was introduced in the Fukui frontier molecular orbital theory [33], is by far the most important local (site) reactivity (selectivity) index. It was introduced by Parr and Yang [35] and it serves a central role in conceptual DFT. The condensed Fukui function, which is a simplification of reducing a three dimensional function to an atom based number [36,37], can be directly used to identify chemical properties [38,34]. It is also a useful criterion to characterize the site-specific reactivity of an atom in a molecule and thus to predict its role in the molecule [37]. Recently, condensed Fukui functions were calculated based on Hirshfeld charges [34,39,40], leading to reliable values of the condensed Fukui function [41].

The Fukui functions [35]:

$$f(r) = \left(\frac{\partial \rho(r)}{\partial N} \right)_V,$$

where N is the number of electrons, $\rho(r)$ is the electron density and $V(r)$ is the potential acting on an electron due to all the other electrons and nuclei. The condensed Fukui function can be approximated using the atomic population of the i th atom, so that the condensed Fukui function describing electrophilic attack (ionization processes) is given by finite difference as [42]:

$$f_i^- \approx q_i(N) - q_i(N - 1) \quad (1)$$

where $q_i(N)$ and $q_i(N - 1)$ are the atomic populations of atom i in the neutral (N electrons) and ionized ($N - 1$ electrons) species, respectively.

The orbital wavefunctions obtained from the single point calculations were then mapped directly into momentum space, as orbital MDs. Through a Fourier transform, applying the plane wave impulse approximation (PWIA) [43], Born–Oppenheimer approximation and independent particle approximation [44], the overlap between the target-ion in the (e,2e) ionization processes is approximated as an one electron Dyson orbital,

$$\sigma \propto \int d\Omega |\phi_j(\vec{p})|^2.$$

Here \vec{p} is now the momentum of the target electron at the instant of ionization. $\phi_j(p)$ is the Dyson orbital, which was approximated by Kohn–Sham (KS) orbitals [45,46] in the weak coupling approximation. Dyson orbitals represent the changes in electronic structure accompanying the detachment of an electron from a molecule. The mapping over the coordinate space wavefunction into momentum space was implemented using HEMS, which is the latest version of the MOMAP [47] code developed at the University of British Columbia.

3. Result and discussion

3.1 Molecular properties

The B3LYP/TZVP model gives the four A imino tautomers, 7H*cis*, 7H*trans*, 9H*cis* and 9H*trans*, as all possessing the same point group symmetry (C_s) and having the same ground electronic state of X^1A . The optimized structures of the four A imino tautomers in the ground state are shown in figure 1, together with the atom specific Hirshfeld charges. Table 1 reports some important geometric parameters of the structures given in figure 1, as well as some other properties. The relative energy differences (ΔE) among the tautomers are slightly different, depending on the methods employed (B3LYP, RI-MP2 and BP86), as shown in this table. However, the order of relative stability among the tautomers predicted by the models is consistently the same. Proton transfer causes small changes in the energies and geometric properties of these tautomers. For example, the total energy variations of the four A imino tautomers, with respect to the A canonical form (amino-9H), are less than 20 kcal mol^{-1} , suggesting a stability order of 9H*trans* > 7H*cis* > 7H*trans* > 9H*cis* in agreement with Refs. [6,48]. As indicated by the structures of the tautomers in figure 1, the formation of two possible two hydrogen bonds at $H_{(11)} \dots N_{(7)}$ and $H_{(12)} \dots N_{(10)}$ in the 9H*trans* tautomer contributes to lower the total energy of this species; whereas the imino 7H tautomers, 7H*cis* and 7H*trans*, each has only one possible hydrogen bond, $N_{(10)}-H_{(15)}$ for 7H*cis* and $N_{(10)}-H_{(12)}$ for 7H*trans*. However, there is no possible hydrogen bond in tautomer 9H*cis*, therefore it has the highest possible energy in the group.

No substantial variations have been found in the geometry parameters of these tautomers, which is in agreement with our previous studies [6,21,49] and others [50]. Small changes in isotropic properties are also reflected in the geometries of the tautomers, in particular the perimeters of the constituent rings. In table 1, the perimeters of the hexagon rings expand with respect to that of canonical A, whereas the perimeters of pentagon rings apparently shrink, when compared to their counterpart of A amino 9H. The imino 7H tautomer pair exhibits a smaller expansion in R $\$-6\$\$ but a larger reduction in R $\$-5\$\$ than the imino 9H pair. An overall small expansion in the perimeters of the purine rings of the tautomers is also observed: 0.065, 0.067, 0.091 and 0.069 Å, respectively due to the corresponding proton transfer from the amino to imino forms. We note, however some apparent variations in associated angles related to the hexagon ring. The $\angle N_{(3)}C_{(4)}C_{(5)}$ has changed approximately 4° for the proton transfer between the 7H and 9H sites, whereas $\angle C_{(5)}C_{(6)}N_{(10)}$ varies more than 6° for the proton transfer between *cis-trans* of the imino tautomer 7H and/or 9H. It is interesting to note that 9H*cis*, the highest energy tautomer of this group, experiences the largest purine ring expansion of 0.091 Å and possesses the largest dipole moment of 4.65 Debye.$$

The atom specific Hirshfeld charges, Q^H , are also shown in figure 1. Hirshfeld charges indicate the atomic contribution to the molecular charge distribution and together with atomic dipoles, reveal important anisotropic properties of the molecule [51]. The proton transfer does not significantly alter Q^H with respect to conformational changes (i.e. positions of the $=N-H$ bonds in the *cis-* and *trans-*isomers) but apparent local relaxation is observed in the $N_{(7)}-H_{(15)}$ and $N_{(9)}-H_{(14)}$ bond regions. For example, the Q^H s on the $N_{(7)}$ and $N_{(9)}$ sites of the 7H tautomer pair are -0.07 and -0.21 , respectively, for *cis* and *trans*; whereas in the 9H tautomer pair, these Q^H s become -0.22 and -0.08 , respectively for *cis* and *trans*. Similar trends are also found in the mobile proton, $H_{(15)}$, depending on whether the proton bonds with an N atom (0.15) or a C atom (0.07).

An analysis of the condensed Fukui function for tautomers undergoing an electrophilic attack is presented in figure 2, (a) for the N atoms and (b) for the C atoms. The condensed Fukui function, f^- , of the N-atom sites is divided into two clusters: one consisting of the f^- s of the $N_{(10)}$, $N_{(3)}$ and $N_{(1)}$ sites, the other consisting of $N_{(7)}$ and $N_{(9)}$. The f^- s in the first cluster exhibit a linear trend without any substantial differences among the four tautomers, as shown in figure 2(a). However, of all the N sites in this figure, the most electrophilic reactive site is $N_{(10)}$ in the imino fragment, $=N_{(10)}-H$, in which the $C_{(6)}=N_{(10)}$ double bond may be broken to produce covalent bonds. The second most electrophilic reactive site is $N_{(3)}$, due to the existence of the double bond in the $C_{(2)}=N_{(3)}-C_{(4)}$ chain. The saturated $N_{(1)}$ site of the imino tautomers possesses very low f^- , which is similar to the $N_{(7)}$ site in the imino-7H pair in the saturated $C_{(5)}-N_{(7)}(H)-C_{(8)}$ chain and to the $N_{(9)}$ site in the imino-9H pair in the saturated $C_{(4)}-N_{(9)}(H)-C_{(8)}$ chain. In the second cluster, the f^- values are split in opposite directions reflecting the positions of the mobile proton on $N_{(7)}$ or $N_{(9)}$. For example, f^- the values on site $N_{(7)}$ are larger in the imino-9H pair than those in the imino-7H pair, since in the imino-9H pair, an unsaturated double $C_{(5)}=N_{(7)}$ bond is present, whereas the same condensed Fukui functions on site $N_{(9)}$ are larger in the imino-7H pair than those of the imino-9H pair, due to the saturated C-N bonds on this site.

The carbon sites are different, with all the carbon sites being associated with a double bond, either $C=C$ or $C=N$. Among the carbon atom sites, sites $C_{(8)}$ and $C_{(2)}$ are the most reactive to electrophilic attacks whereas site $C_{(6)}$ is the least electrophilic active, as shown in figure 2(b). This suggests that an electrophilic attack on either $C_{(8)}$ or $C_{(2)}$ will saturate the site with single bonds, whereas the $C_{(6)}$ site may be able to form another double bond with $N_{(1)}$ in the hexagon ring, thereby reducing the reactivity. It is obvious that site $C_{(8)}$ of the imino-9H tautomers is the most electrophilic reactive site. The high reactivity of this exposed $C_{(8)}$ site might lead it to be a potential DNA damage hot-spot, as also noted by Gu *et al.* [50] and

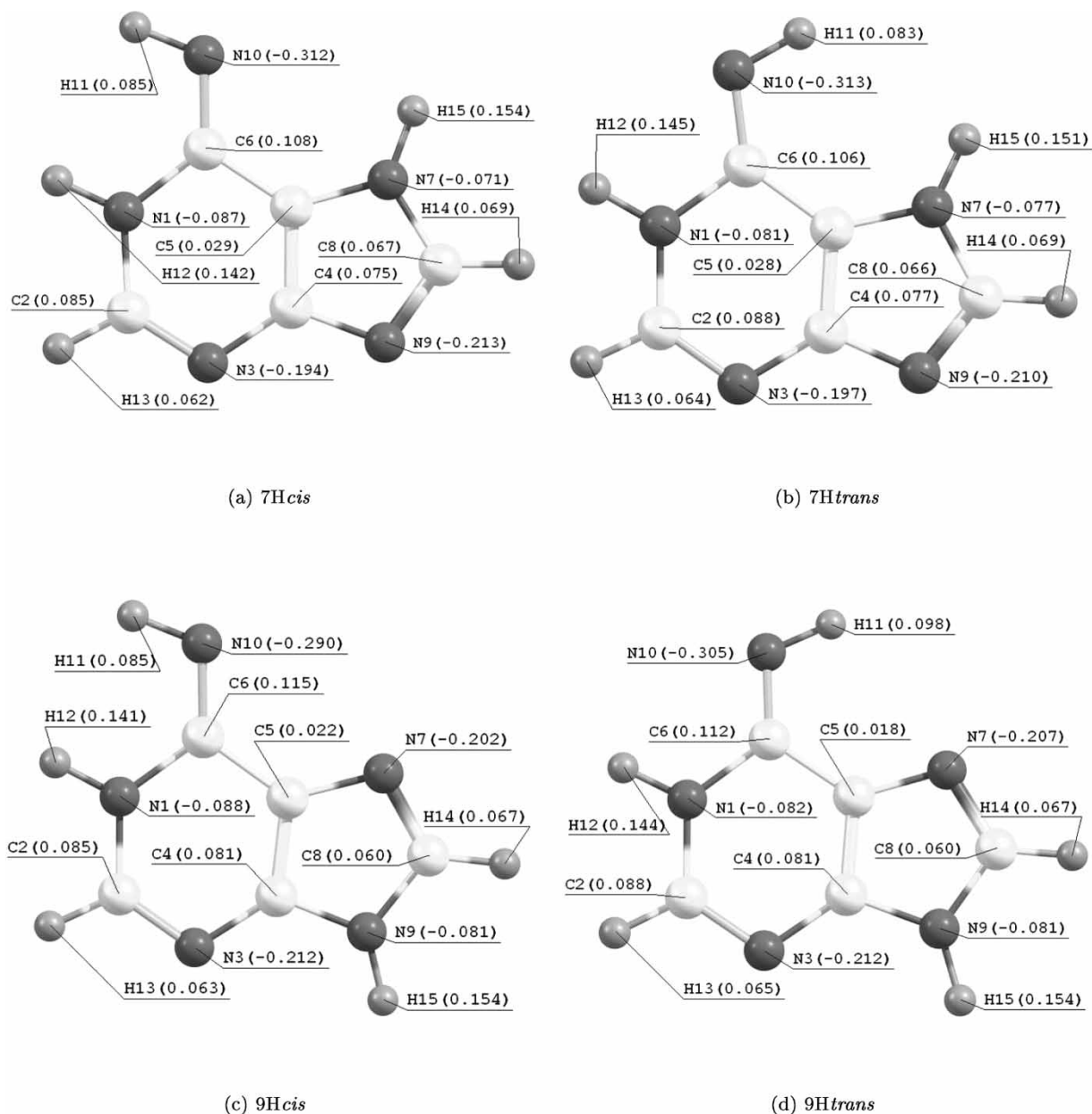


Figure 1. Optimized ground state (X^1A) geometries of the four A imino tautomers. Hirshfeld atomic charges are given in parenthesis.

Table 1. Relative Energies (kcal/mol), molecular dipole moments μ (Debye) and perimeters (\AA) of the pentagon, hexagon and purine rings [21] of the A imino tautomers.

Tautomer	ΔE (kcal/mol)			μ (Debye)	Ring perimeter (\AA)		
	This work [†]	RI-MP2/TZVPP [‡]	BP86/TZ2P [§]		R_5	R_6	R_p [§]
Amino 9H	0	0	0	2.45	6.850	8.162	15.022
Imino 7Hcis	16.15	16.09	14.7	3.56	6.804	8.273	15.077
Imino 7Htrans	16.43	16.55	14.9	3.21	6.814	8.265	15.079
Imino 9Hcis	18.46	18.53	17.0	4.65	6.811	8.292	15.103
Imino 9Htrans	13.80	12.07	10.9	3.94	6.810	8.271	15.081

[†] B3LYP/TZVP model.

[‡] See Ref. [48].

[§] See Ref. [6].

[§] see Ref. [21]. Here $R_p = R_5 + R_6$.

^{||} A canonical form (global minimum structure).

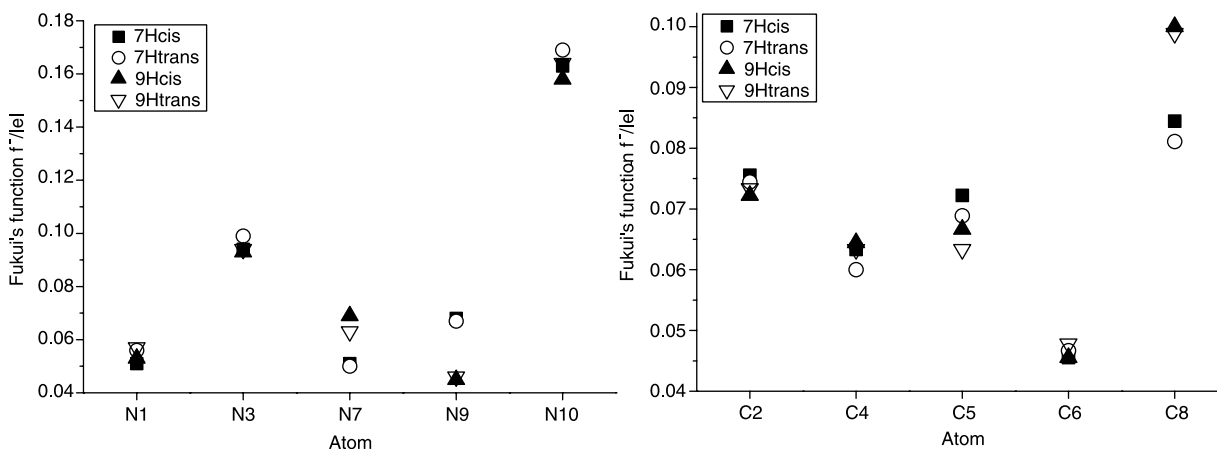


Figure 2. Distribution of the condensed Fukui functions (f^-) at the nitrogen (a) and carbon (b) sites in the A tautomers.

Breimer [52]. Though there is a small difference in f^- between sites $C_{(4)}$ and $C_{(5)}$, the double $C_{(4)}=C_{(5)}$ bonds of the imino tautomers are unlikely to break under electrophilic attacks due to their positions in three dimensional space.

3.2 Ionization spectra and orbital momentum distributions

The ground state (X^1A) configurations of all the tautomers consist of 15 doubly occupied molecular orbitals (MOs) in the outer valence space, ... $(21a')$ $(22a')$ $(23a')$ $(1a'')$ $(24a')$ $(25a')$ $(26a')$ $(2a'')$ $(3a'')$ $(27a')$ $(4a'')$ $(5a'')$ $(28a')$ $(29a')$ $(6a'')$ HOMO).

The vertical ionization energies in the outer valence space of the tautomers have been calculated using a number of quantum mechanical models including RHF/TZVP, B3LYP/TZVP, OVGf/TZVP and SAOP/TZ2P, as reported in figure 3. While the orbital energies generated using DFT models such as B3LYP/TZVP do not produce quantitative vertical ionization energies, the DFT based SAOP/TZ2P model

and the Green's function model OVGf/TZVP agree well with a recent experiment [53] (note that the experimental data is dominated by the A canonical form). The orbital energies obtained from the RHF/TZVP and B3LYP/TZVP models, shown in this figure, however, provide references of the electron correlation and electron relaxation effects. The clear "kink" between MO7 ($27a'$) and MO8 ($3a''$) in the outer valence ionization spectrum suggests larger electron correlation and relaxation effects, as well as increasing many-body effects when the hole moves inwards. Table 2 lists the outer valence orbital vertical ionization energies of the four tautomers obtained using the SAOP/TZ2P and OVGf/TZVP models. The orbital ionization energies are more congested, in general, in the imino-9H pair rather than in the imino-7H pair. Nevertheless, the outer valence ionization energies of the tautomers do not experience any substantial changes with regard to the proton transfer.

Ionization energy alone is insensitive to proton transfer processes, and the existence of tautomers under experimental condition often causes the congested spectra difficult to analyze [53]. Position space based anisotropic

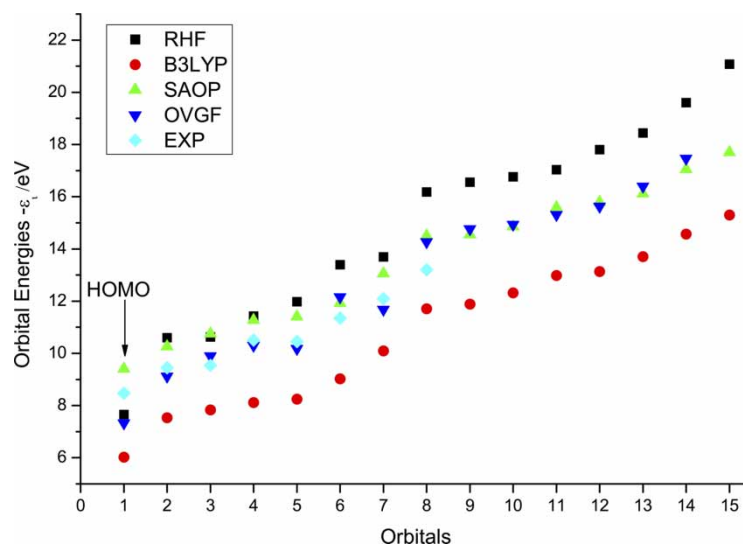


Figure 3. A comparison of vertical ionization energies (eV) in the outer valence space of the imino 9Htrans A tautomer.

Table 2. Outer valence orbital energies (eV) of the A tautomers.

MO	Sym.	7Hcis		7Htrans		9Hcis		9Htrans		ADC(3)/6-31G [†]	Exp [‡]
		SAOP [‡]	OVGF [¶]	SAOP [‡]	OVGF [¶]	SAOP [‡]	OVGF [¶]	SAOP [‡]	OVGF [¶]		
1	6a''	9.56	7.90	9.59	7.92	9.40	7.32	9.40	7.33	7.93	8.48
2	29a'	10.65	9.87	10.55	9.89	10.43	9.82	10.26	9.12	9.20	9.6
3	28a'	10.84	10.39	10.95	10.54	10.62	9.18	10.75	9.90	10.23	9.6
4	5a''	11.15	10.05	11.22	9.95	11.22	10.24	11.27	10.30	9.36	10.5
5	4a''	11.52	10.24	11.59	10.44	11.38	9.99	11.41	10.17	10.26	10.5
6	27a'	11.53	11.10	11.56	11.16	11.85	12.13	11.92	12.16	11.20	11.39
7	3a''	13.16	12.41	13.20	12.41	13.05	11.57	13.06	11.68	12.09	12.1
8	26a'	14.49	14.12	14.48	14.11	14.24	14.34	14.55	14.27		13.21
9	2a''	14.56	14.47	14.64	14.43	14.51	14.26	14.5	14.77	13.54	
10	25a'	14.79	15.00	15.10	15.14	14.84	14.86	14.86	14.94		
11	24a'	15.47	15.71	15.82	15.54	15.22	15.19	15.59	15.31		
12	1a''	15.81	15.50	15.91	16.072	15.77		15.79	15.63		
13	23a'	16.69	17.11	16.37	16.60	16.61	16.80	16.12	16.40		
14	22a'	17.16	17.67	17.10	17.50	17.26	17.60	17.06	17.47		
15	21a'	17.83	18.23	17.78	18.25	17.70		17.70			

[†] Results for A canonical form (amino 9H) [53].

[‡] Basis set TZ2P.

[¶] Basis set TZVP.

properties provide information either for the entire molecule (e.g. dipole moments) or are atom based (e.g. Hirshfeld charges and condensed Fukui functions), which cannot differentiate proton location of *cis/trans* imino tautomers. To this regard, DSA [23] is applied here in order to obtain orbital based chemical bonding information from momentum space, applying the theory [43] underlining electron momentum spectroscopy.

The MOs in the outer valence space, for the A tautomers with C_s symmetry, are obtained from two independent Hamiltonian matrices of the B3LYP/TZVP model: *a'* (nine MOs) and *a''* (six MOs). The anti-symmetric MOs of *a''* symmetry contain the purine plane (*xy*-plane) as a nodal plane, so that they form π MOs dominated by the

$2p_z$ -atomic orbitals (AOs) of the C and N atoms. Proton transfer on the purine plane is, therefore, unlikely to cause any substantial changes in these MOs, including the HOMO (6a''). The orbital MDs of the HOMOs (6a'') of the four imino tautomers, as reported in figure 4, quantitatively demonstrate that the HOMOs are nearly identical. The contours of these four HOMOs suggest the similarities in the tautomers on this MO: each of the anti-symmetric π -like electron density distributions is formed by four partitions in a similar manner. That is, the amine group (=NH), H-C₍₂₎-N₍₃₎, N₍₇₎(H)-C₍₈₎-H and the central chain formed by H-N₍₁₎-C₍₆₎-C₍₄₎-C₍₅₎. Such a partition pattern leaves all the N₍₉₎(H) sites on the nodal "plane", which divides the N₍₁₎-C₍₆₎-C₍₄₎-C₍₅₎

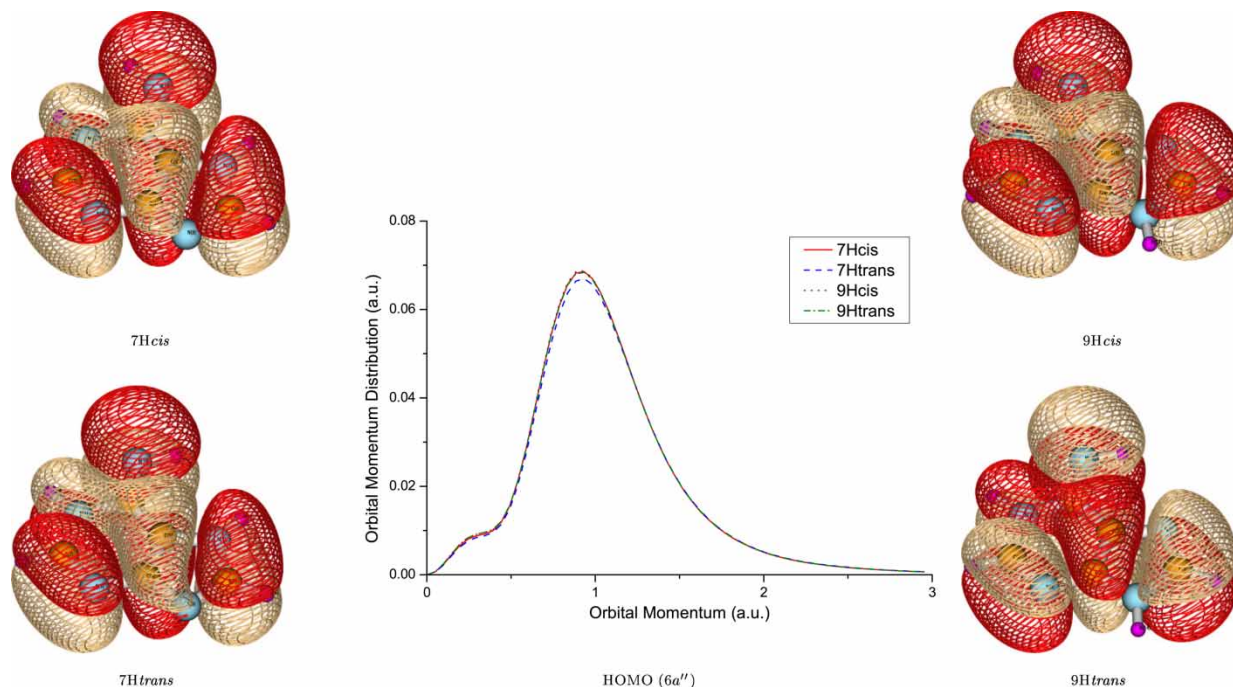


Figure 4. The HOMOs (orbital 6a'') of the four imino A tautomers.

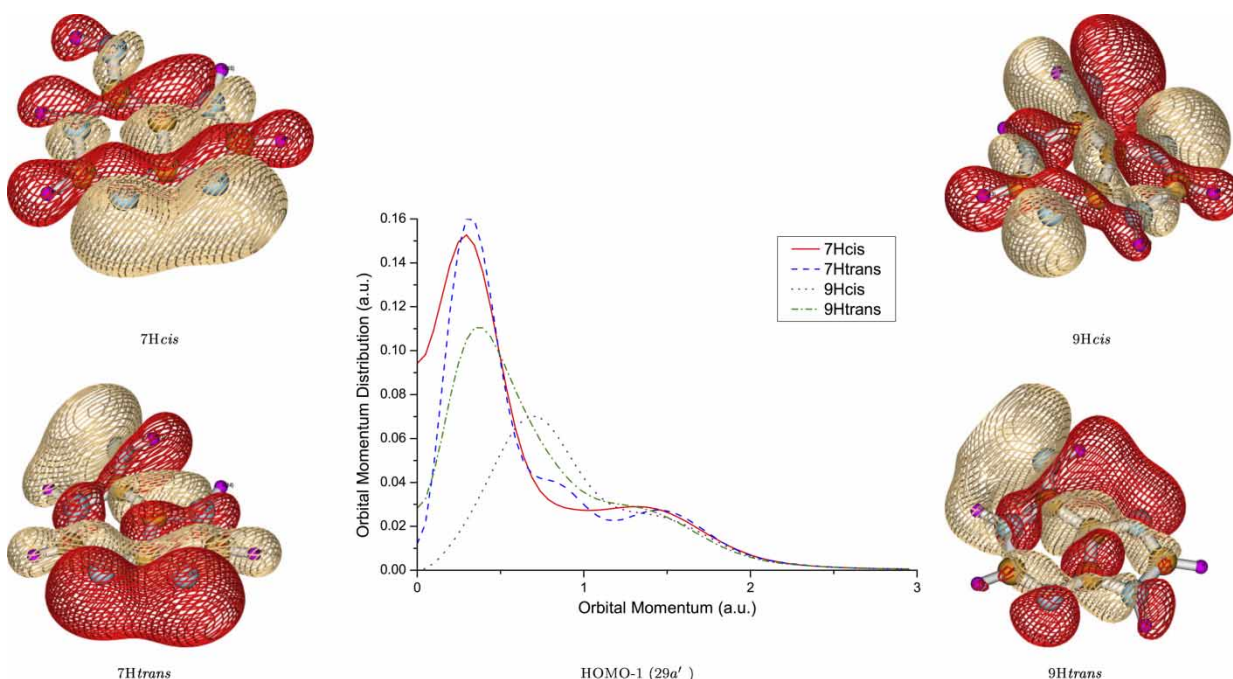


Figure 5. The NHOMOs (or HOMO-1, orbital $29a'$) of the four imino A tautomers, which is the most important signature orbital of the A imino tautomers.

and $N_{(7)}(H)-C_{(8)}-H$ fragments. In addition, the proton attached to $N_{(7)}$ in the 7H tautomer pair is “absorbed” in the fragment of $N_{(7)}(H)-C_{(8)}$. As a result, proton transfer between the 7H and 9H A tautomers is not significant in the HOMO. On the other hand, the imine group ($=N-H$) in the HOMOs is also separated by a nodal “plane”, which effectively isolates the imine functional group. As a consequence, differences in the proton positions in *cis*- and *trans*-configurations are also minimized in the HOMOs. The common nature in bonding of the HOMOs is reflected in the respective orbital MDs, with a strong π bond nature also being indicated by the bell shaped orbital MDs [54].

It is the in-plane σ dominated orbitals which contribute significantly to proton transfer [21,22,49]. Thus, to recognize proton transfer in the tautomers, such as *trans/cis* and imino-7H/imino-9H, information from in-plane orbitals related to the σ -bonds ought to be the target of our analysis. In a quantitative screen of the outer valence space MOs with a' symmetry, using their orbital MDs, it is found that the σ dominated orbitals are indeed substantially more sensitive to the proton transfer than their π dominated counterparts. However, not all such σ dominated MOs are subject to the same degree of response. Nevertheless, using DSA [23], we are able to identify the orbital based response to different proton transfer processes in these tautomers: (1) the proton transfer impact on the entire purine plane (e.g. HOMO-1, orbital $29a'$); (2) proton transfer within the purine ring, such as imino-7H/imino-9H (e.g. orbital $27a'$) and (3) proton transfer within the amine group, such as *trans/cis*, (e.g. orbital $22a'$).

Three in-plane σ orbitals $29a'$ (HOMO-1 or NHOMO), $27a'$ and $22a'$ of A are therefore highlighted as the orbital

response to such proton transfer processes. Figure 5 gives the momentum space orbital MDs of the HOMO-1 orbitals (orbital $29a'$) of the four tautomers, together with their position space orbital contours. As seen from the information provided in the figure, unlike the HOMOs of the species, which exhibit remarkable similarities, the HOMO-1 orbitals of the same species display minimal similarities. The orbital ($29a'$) electron density and MDs suggest that the bonding mechanisms of the tautomers are distinctly different from each other and from their HOMO counterparts. These orbital MDs indicate that this MO is dominated by a hybridized bonding nature, as the shape of the orbital MDs is more or less a combination of a bell-shaped π bonding nature and a half-bell-shaped σ bond nature [54]. Some local similarities can also be recognized from the orbital contours. For example, the electron overlap between the electron lone pairs of $N_{(3)}(H)$ and $N_{(9)}$ in the 7H*cis* and 7H*trans* A tautomer pair is apparent. The proton transfer in *trans/cis* of the 7H pair (left side contours of figure 5) concentrates in the local region consisting of the $H-N_{(1)}-C_{(6)}-C_{(5)}$ and $=N-H$ fragments. The possible hydrogen bonds between $H_{(12)}$ and $N_{(10)}$ in the *trans*-imino tautomer pair of 7H*trans* and 9H*trans* are also observed. In addition, the second hydrogen bond between $H_{(11)}$ and $N_{(7)}$ in the 9H*trans* tautomer is also seen. This observation in HOMO-1 supports our earlier interpretation as to why this tautomer structure (9H*trans*) yields the lowest total energy amongst the tautomers under study.

Orbital $27a'$, given in figure 6, highlights the proton transfer between imino-7H/imino-9H. As indicated by the orbital MDs of the imino-7H pair and imino-9H pair, the most significant changes which differentiate the proton

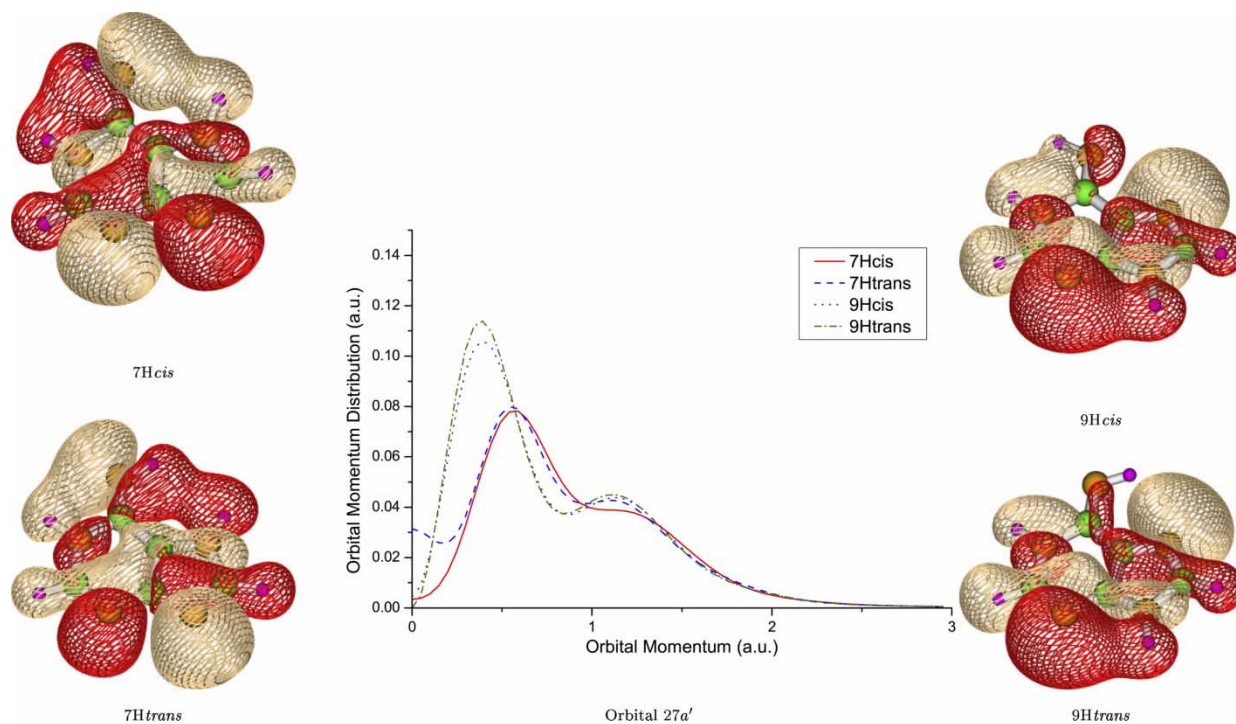


Figure 6. Orbital based response (orbital $27a'$) of the proton transfer among the A imino tautomers. This orbital reveals the proton transfer between the purine ring of the $N_{(7)}$ and $N_{(9)}$ sites.

positions in this orbital are between $N_{(7)}$ and $N_{(9)}$. For the imino-9H pair, the *cis* or *trans* positions of the proton exhibit little impact on the orbital MDs—the two tautomers having almost identical orbital MDs. Significant similarities are also observed in the orbital density distributions of the pair (right side of the figure), where *cis/trans* proton transfer in the imino-9H pair has limited and local effects on the orbital, since the imino group is significantly less populated. Similar to the imino-9H pair, the imino-7H pair also shows a large degree of similarities

in either momentum space or position space. Some small differences in the lower momentum region of $\mathbf{p} < 0.25$ a.u. are observed which reflect the two “peanut shell shaped” density contours of $H_{(12)} \dots C_{(6)} \dots H_{(11)}$ and $N_{(10)} \dots H_{(15)}$ in 7Hcis and $H_{(15)} \dots C_{(6)} \dots H_{(11)}$ and $N_{(10)} \dots H_{(12)}$ in 7Htrans.

Orbital $22a'$ represents the *cis-trans* signature in the tautomers. When both are *cis* or *trans*, substantial similarities between the imino 7H and imino 9H tautomer pair are revealed in the orbital MDs and orbital contour

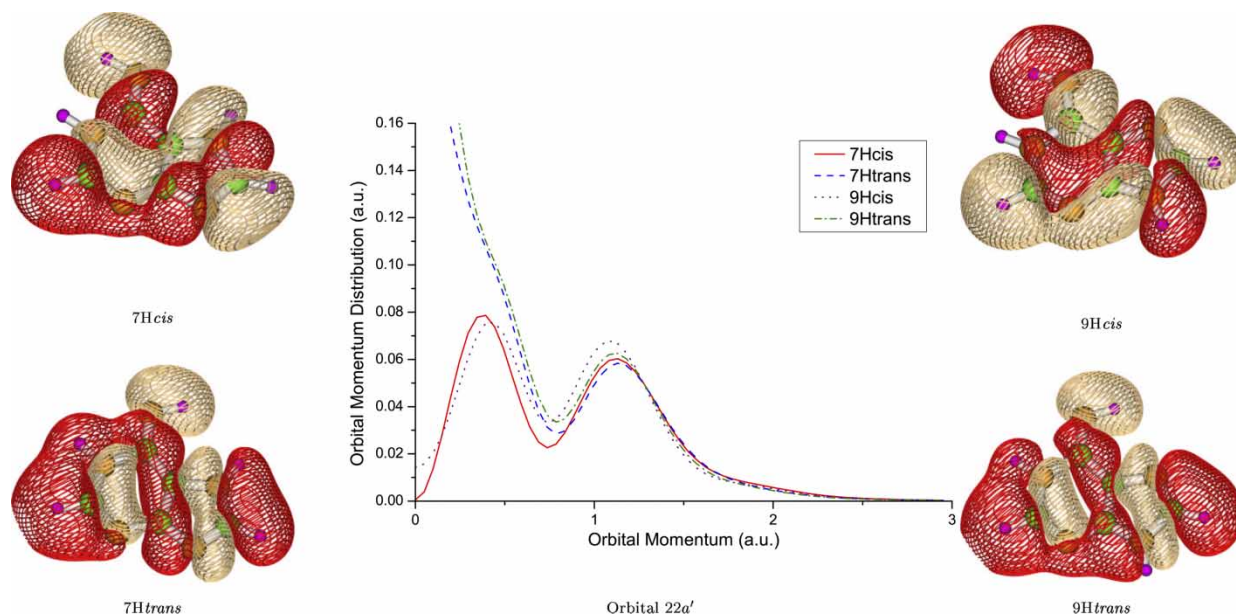


Figure 7. Orbital based response (orbital $22a'$) of the proton transfer among the A imino tautomers. This orbital indicates the direction (*cis-trans*) of the flag proton in the imino group ($=N-H$) of $N_{(10)}$.

plots, as given in figure 7. This orbital certainly demonstrates that the *cis*–*trans* proton transfer processes are not small perturbations, but have a profound impact on the electronic structures. The *cis* pair, which has more of a *p*-electron domination, shows a layer structure in their contours where the purine ring is organized as a whole. In the *trans* tautomer pair, there is a similar pattern in the contours in which the purine ring contains either “n” or “u” shapes formed by the hexagon, together with a pair of “peanut shells” which are contributions from the pentagon. The proton transfer between the N₍₇₎ and N₍₉₎ sites determines “n” (N₍₇₎) or “u” (N₍₉₎). Moreover in this tautomer pair, all the hydrogen *s* orbitals make significant contributions to orbital 22*d'* in the *trans* pair. As a result, the corresponding orbital MDs contain apparent *s* contributions as shown in the region of momentum <0.75 a.u.

4. Conclusions

Intramolecular proton transfer among the 7H*cis*, 7H*trans*, 9H*cis* and 9H*trans* A tautomers has been studied on an atom base and an orbital base, using density functional theory (B3LYP/TZVP, SAOP/TZ2P, LB94/TZ2P) and Green function (OVGF/TZVP) models. Though the differences are small, the total energies of the four tautomers suggested the stability order of the tautomers might be 9H*trans* > 7H*cis* > 7H*trans* > 9H*cis*, due to possible hydrogen bonds. Insignificant geometric changes, but apparent dipole moment differences, among the tautomers suggest an alternative anisotropic property related analysis may be more appropriate to reveal the proton transfer processes. Hirshfeld atomic charges and condensed Fukui function (f^-) are thus employed as a consequence. The Hirshfeld atomic charges indicate that significant local charge redistributions occur in the proton attaching to either N₍₇₎ or N₍₉₎, reflecting the sensitivity of Hirshfeld charges to the 7H/9H proton transfer. Similarly, the condensed Fukui function is also sensitive to the atom based 7H/9H proton transfer. In addition, the condensed Fukui function provides information on the order of the electrophilic reactive sites. Accordingly, the imino nitrogen site, N₍₁₀₎ is the most likely to attract electrophilic attack. For the carbon atoms, this site is C₍₈₎ in agreement with existing literature.

Vertical ionization spectra and orbital MDs of the outer valence space are then calculated. The vertical ionization energies are generally consistent with the experimentally available data of canonical A (A amino 9H). Applying DSA [23], we confirmed previous conclusions on planar molecules that the π bond related orbitals (a'') are insensitive to proton transfer processes [21,22] and it is the in-plane σ bonds which reveal proton transfers. As the highest occupied MOs of the purine tautomers possess a'' symmetry (assumed planar), these HOMOs remain insensitive for proton transfers, which supports our previous conclusion [25,55] that not all chemical reactions

occur in the frontier orbitals. Moreover, orbital based responses to various proton transfers are presented: orbital 29*d'* (HOMO-1) is a signature orbital differentiating all the four tautomers; orbital 27*d'* is a site (N₍₇₎ and N₍₉₎) specific orbital, whereas orbital 22*d'* reveals that the proton positions on the imine group =N–H is not a local effect, but significantly alters the orbital density patterns of the entire molecule.

Acknowledgements

This research is partially supported by the Australian Research Council (ARC) and a Vice-Chancellor’s Research Strategic Initiative Grant of Swinburne University of Technology. The authors acknowledge the Australian Partnership for Advanced Computing (APAC) for use of the National Supercomputing Facilities.

References

- [1] J.D. Watson, F.H.C. Crick. A structure for deoxyribonucleic acid. *Nature*, **171**, 737 (1953).
- [2] S.A. Smith, B.P. Engelward. *In vivo* repair of methylation damage in Aag 3-methyladenine DNA glycosylase null mouse cells. *Nucleic Acids Res.*, **28**, 3294 (2000).
- [3] L. Sanche. Nanoscopic aspects of radiobiological damage: fragmentation induced by secondary low-energy electrons. *Mass Spectrom. Rev.*, **21**, 349 (2003).
- [4] B. Boudaiffa, P. Cloutier, D. Hunting, M.A. Huels, L. Sanche. Resonant formation of DNA strand breaks by low-energy (3 to 20 eV) electrons. *Science*, **287**, 1658 (2000).
- [5] M.A. Huels, B. Boudaiffa, P. Cloutier, D. Hunting, L. Sanche. Single, double, and multiple double strand breaks induced in DNA by 3–100 eV electrons. *J. Am. Chem. Soc.*, **125**, 4467 (2003).
- [6] C. Fonseca Guerra, F.M. Bickelhaupt, S. Saha, F. Wang. Adenine tautomers: relative stabilities, ionization energies, and mismatch with cytosine. *J. Phys. Chem. A*, **110**, 4012 (2006).
- [7] P.O. Lowdin. Isotope effect in tunneling and its influence on mutation rates. *Adv. Quantum Chem.*, **2**, 213 (1965).
- [8] H. Robinson, Y.G. Gao, C. Bauer, C. Roberts, C. Switzer, A.H. Wang. 2'-Deoxyisoguanosine adopts more than one tautomer to form base pairs with thymidine observed by high-resolution crystal structure analysis. *J. Biochem.*, **37**, 10897 (1998).
- [9] T. Chatake, T. Hikima, A. Ono, Y. Ueno, A. Matsuda, A. Takenaka. Crystallographic studies on damaged DNAs. II. N-6-methoxyadenine can present two alternate faces for Watson–Crick base-pairing, leading to pyrimidine transition mutagenesis. *J. Mol. Biol.*, **294**, 1223 (1999).
- [10] R. Ramaekers, L. Adamowicz, G. Maes. Tautomerism and H-bonding characteristics of 2-aminopurine: a combined experimental and theoretical study. *Eur. Phys. J. D*, **20**, 375 (2002).
- [11] J. Gu, J. Leszczynski. A DFT study of the water-assisted intramolecular proton transfer in the tautomers of adenine. *J. Phys. Chem. A*, **103**, 2744 (1999).
- [12] D.C. Lührs, J. Viallon, I. Fischer. Excited state spectroscopy and dynamics of isolated adenine and 9-methyladenine. *Phys. Chem. Chem. Phys.*, **3**, 1827 (2001).
- [13] O.S. Sukhanov, O.V. Shishkin, L. Gorb, Y. Podolyan, J. Leszczynski. Molecular structure and hydrogen bonding in polyhydrated complexes of adenine: a DFT study. *J. Phys. Chem. B*, **107**, 2846 (2003).
- [14] J.P. García-Terán, O. Castillo, A. Luque, U. García-Couceiro, G. Beobide, P. Román. Supramolecular architectures assembled by the interaction of purine nucleobases with metal-oxalato frameworks. Non-covalent stabilization of the 7H-adenine tautomer in the solid-state. *Dalton Trans.*, **7**, 902 (2006).
- [15] A.K. Vrkic, T. Taverner, P.F. James, R.A.J. O’Hair. Gas phase ion chemistry of biomolecules, part 38. Gas phase ion chemistry of

- charged silver(I) adenine ions via multistage mass spectrometry experiments and DFT calculations. *Dalton Trans.*, **2**, 197 (2004).
- [16] A.Yu. Rubina, Y.V. Rubin, V.A. Sorokin, M.K. Shukla, J. Leszczynski. Complexes of adenine with metal ions: stability and excited states. *Pol. J. Chem.*, **79**, 2005 (1873).
- [17] J.V. Burda, J. Šponer, J. Leszczynski. The interactions of square platinum(II) complexes with guanine and adenine: a quantum-chemical *ab initio* study of metalated tautomeric forms. *J. Biol. Inorg. Chem.*, **5**, 178 (2000).
- [18] C. Plützer, K. Kleinermanns. Tautomers and electronic states of jet-cooled adenine investigated by double resonance spectroscopy. *Phys. Chem. Chem. Phys.*, **4**, 4877 (2002).
- [19] K.B. Wiberg, P.R. Rablen. Comparison of atomic charges derived via different procedures. *J. Comput. Chem.*, **14**, 1504 (1993).
- [20] J. Elguero, A.R. Katritzky, O. Denisko. *Heterocyclic Chemistry*, A.R. Katritzky (Ed.), Volume 76, Academic Press, San Diego (2000).
- [21] F. Wang, M. Downton, N. Kidwani. Adenine tautomer electronic structural signatures studied using dual space analysis. *J. Theor. Comput. Chem.*, **4**, 247 (2005).
- [22] D.B. Jones, F. Wang, D.A. Winkler, M.J. Brunger. Orbital based electronic structural signatures of the guanine keto G-7H/G-9H tautomer pair as studied using dual space analysis. *Biophys. Chem.*, **121**, 105 (2006).
- [23] F. Wang. Assessment of quantum mechanical models based on resolved orbital momentum distributions of *n*-butane in the outer valence shell. *J. Phys. Chem. A*, **107**, 10199 (2003).
- [24] C.T. Falzon, F. Wang. Understanding glycine conformation through molecular orbitals. *J. Chem. Phys.*, **123**, 214307 (2005).
- [25] C.T. Falzon, F. Wang. Conformational processes in L-alanine studied using dual space analysis. *International Conference on Computational Science (ICCS 2006)*, V. Alexandrov, D. van Albada, P. Sloot, J. Dongarra (Eds.), LNCS, Springer (2006).
- [26] P.R.T. Schipper, O.V. Gritsenko, S.J.A. van Gisbergen, E.J. Baerends. Molecular calculations of excitation energies and (hyper)polarizabilities with a statistical average of orbital model exchange-correlation potentials. *J. Chem. Phys.*, **112**, 1344 (2000).
- [27] D.P. Chong. Augmenting basis set for time-dependent density functional theory calculation of excitation energies: Slater-type orbitals for hydrogen to krypton. *Mol. Phys.*, **103**, 749 (2005).
- [28] R. van Leeuwen, E.J. Baerends. Exchange-correlation potential with correct asymptotic-behavior. *Phys. Rev. A*, **49**, 2421 (1994).
- [29] L.S. Cederbaum, W. Domcke. Theoretical aspects of ionization potentials and photoelectron spectroscopy: a Green's function approach. *Adv. Chem. Phys.*, **36**, 206 (1977).
- [30] M.J. Frisch, G.W. Trucks, H.B. Schlegel, G.E. Scuseria, M.A. Robb, J.R. Cheeseman Jr., J.A. Montgomery, T. Vreven, K.N. Kudin, J.C. Burant, J.M. Millam, S.S. Iyengar, J. Tomasi, V. Barone, B. Mennucci, M. Cossi, G. Scalmani, N. Rega, G.A. Petersson, H. Nakatsuji, M. Hada, M. Ehara, K. Toyota, R. Fukuda, J. Hasegawa, M. Ishida, T. Nakajima, Y. Honda, O. Kitao, H. Nakai, M. Klene, X. Li, J.E. Knox, H.P. Hratchian, J.B. Cross, V. Bakken, C. Adamo, J. Jaramillo, R. Gomperts, R.E. Stratmann, O. Yazyev, A.J. Austin, R. Cammi, C. Pomelli, J.W. Ochterski, P.Y. Ayala, K. Morokuma, G.A. Voth, P. Salvador, J.J. Dannenberg, V.G. Zakrzewski, S. Dapprich, A.D. Daniels, M.C. Strain, O. Farkas, D.K. Malick, A.D. Rabuck, K. Raghavachari, J.B. Foresman, J.V. Ortiz, Q. Cui, A.G. Baboul, S. Clifford, J. Cioslowski, B.B. Stefanov, G. Liu, A. Liashenko, P. Piskorz, I. Komaromi, R.L. Martin, D.J. Fox, T. Keith, M.A. Al-Laham, C.Y. Peng, A. Nanayakkara, M. Challacombe, P.M.W. Gill, B. Johnson, W. Chen, M.W. Wong, C. Gonzalez, J.A. Pople. *Gaussian 03, Revision C.02*, (2004).
- [31] E.J. Baerends, J. Autschbach, A. Bérces, C. Bo, P.M. Boerrigter, L. Cavallo, D.P. Chong, L. Deng, R.M. Dickson, D.E. Ellis, M. van Faassen, L. Fan, T.H. Fischer, C. Fonseca Guerra, S.J.A. van Gisbergen, J.A. Groeneveld, O.V. Gritsenko, M. Grüning, F.E. Harris, P. van den Hoek, H. Jacobsen, L. Jensen, G. van Kessel, F. Kootstra, E. van Lenthe, D.A. McCormack, A. Michalak, V.P. Osinga, S. Patchkovskii, P.H.T. Philipsen, D. Post, C.C. Pye, W. Ravenek, P. Ros, P.R.T. Schipper, G. Schreckenbach, J.G. Snijders, M. Solà, M. Swart, D. Swerhone, G. te Velde, P. Vermoortels, L. Versluis, O. Visser, F. Wang, E. van Wezenbeek, G. Wiesenekker, S.K. Wolff, T.K. Woo, L. Yakovleva, T. Ziegler. *Adf2004.01*, (2004).
- [32] F.L. Hirshfeld. Bonded-atom fragments for describing molecular charge densities. *Theor. Chem. Acta*, **44**, 129 (1977).
- [33] K. Fukui. Role of frontier orbitals in chemical reactions. *Science*, **218**, 747 (1982).
- [34] F. De Proft, C. Van Alsenoy, A. Peeters, W. Langenaeker, P. Geerlings. Atomic charges, dipole moments, and Fukui functions using the Hirshfeld partitioning of the electron density. *J. Comput. Chem.*, **23**(12), 1198 (2002).
- [35] R.G. Parr, W. Yang. Density functional approach to the frontier-electron theory of chemical reactivity. *J. Am. Chem. Soc.*, **106**, 4049 (1984).
- [36] F. Gilardoni, J. Weber, H. Chermette, T.R. Ward. Reactivity indices in density functional theory: a new evaluation of the condensed Fukui function by numerical integration. *J. Phys. Chem. A*, **102**, 3607 (1998).
- [37] W. Tiznado, E. Chamorro, R. Contreras, P. Fuentealba. Comparison among four different ways to condense the Fukui function. *J. Phys. Chem. A*, **109**, 3220 (2005).
- [38] P.K. Chatteraj, U. Sarkar, D.R. Roy. Electrophilicity index. *Chem. Rev.*, **106**, 2065 (2006).
- [39] R.K. Roy, S. Pal, K. Hirao. On non-negativity of Fukui function indices. *J. Chem. Phys.*, **110**(17), 8236 (1999).
- [40] R.K. Roy, K. Hirao, S. Pal. On non-negativity of Fukui function indices. II. *J. Chem. Phys.*, **113**(4), 1372 (2000).
- [41] J.L. Gazquez, A. Cedillo, B. Gomez, A. Vela. Molecular fragments in density functional theory. *J. Phys. Chem. A*, **110**(13), 4535 (2006).
- [42] W. Yang, W.J. Mortier. The use of global and local molecular parameters for the analysis of the gas-phase basicity of amines. *J. Am. Chem. Soc.*, **108**, 5708 (1986).
- [43] E. Weigold, I.E. McCarthy. *Electron Momentum Spectroscopy*, Kluwer-Academic, USA (1999).
- [44] I.E. McCarthy, E. Weigold. Electron momentum spectroscopy of atoms and molecules. *Rep. Prog. Phys.*, **54**, 789 (1991).
- [45] P. Duffy, D.P. Chong, M.E. Casida, D.R. Salahub. Assessment of Kohn-Sham density-functional orbitals as approximate Dyson orbitals for the calculation of electron-momentum-spectroscopy scattering cross-sections. *Phys. Rev. A*, **50**, 4707 (1994).
- [46] O. Dolgounitcheva, V.G. Zakrzewski, J.V. Ortiz. Electron propagator theory of guanine and its cations: tautomerism and photoelectron spectra. *J. Am. Chem. Soc.*, **122**, 12304 (2000).
- [47] C.E. Brion. Looking at orbitals in the laboratory: the experimental investigation of molecular wavefunctions and binding energies by electron momentum spectroscopy. *Int. J. Quantum Chem.*, **29**, 1397 (1989).
- [48] M. Hanus, M. Kabelac, J. Rejnek, F. Ryjacek, P. Correlated *ab initio* study of nucleic acid bases and their tautomers in the gas phase, in a microhydrated environment, and in aqueous solution. Part 3. Adenine. *J. Phys. Chem. B*, **108**, 2087 (2004).
- [49] M. Downton, F. Wang. Differentiation of adenine non-planarity in valence molecular orbitals. *Mol. Simul.*, **32**, 667 (2006).
- [50] J. Gu, A. Tian, W.K. Lee, N.B. Wong. Intramolecular proton transfer in the tautomers of C8 oxidative adenine: a DFT study. *J. Phys. Chem. A*, **104**, 10692 (2000).
- [51] F. Wang, W.N. Pang, M. Huang. Valence space electron momentum spectroscopy of diborane. *J. Electron Spectrosc. Relat. Phenom.*, **151**, 215 (2006).
- [52] L.H. Breimer. Enzymatic excision from-irradiated polydeoxyribonucleotids of adenine residues whose imidazole rings have been ruptured. *Nucleic Acids Res.*, **12**, 6359 (1984).
- [53] A.B. Trofimov, J. Schirmer, V.B. Kobychew, A.W. Potts, D.M.P. Holland, L. Karlsson. Photoelectron spectra of the nucleobases cytosine, thymine and adenine. *J. Phys. B At. Mol. Opt. Phys.*, **39**, 305 (2006).
- [54] F. Wang, M.J. Brunger, I.E. McCarthy, D.A. Winkler. Exploring the electronic structure of 2,6-stelladione from momentum space I: the p-dominant molecular orbitals in the outer valence shell. *Chem. Phys. Lett.*, **382**, 217 (2003).
- [55] S. Saha, F. Wang, C.T. Falzon, M.J. Brunger. Coexistence of 1,3-butadiene conformers in ionization energies and Dyson orbitals. *J. Chem. Phys.*, **123**, 124315 (2005).

Copyright of *Molecular Simulation* is the property of Taylor & Francis Ltd and its content may not be copied or emailed to multiple sites or posted to a listserv without the copyright holder's express written permission. However, users may print, download, or email articles for individual use.